encit 2020

ABCM Associação Brasileira de Engenharia e Ciências Mecânicas

18th Brazilian Congress of Thermal Sciences and Engineering
November 16–20, 2020 (Online)

ENC-2020-0089
HIGH-TEMPERATURE ENERGY STORAGE SYSTEMS WITH NANOFLUIDS

Caroline Fernandes Farias
Guilherme Borges Ribeiro
Instituto Tecnológico de Aeronáutica – Departamento de Engenharia Mecânica
farias.caroline@hotmail.com, gbribeiro@ita.br

Abstract. *Nuclear reactors are commonly subject to significant variable energy demands. These variable energy requirements can negatively affect the effective capacity factor of the reactor and result in severe penalties with the waste and inefficient use of fissile fuel. Coupling a nuclear reactor to a thermal energy storage system can enable the use of nuclear energy in power and propulsion systems more reasonably. The nuclear reactor can operate at a constant power level, supplying heat to the TES (Thermal Energy Storage), which can supply the power system, as required, rapidly responding to variations in demand without overloading the control system. Nonetheless, the linkage results not only increased the safety of the energy conversion system but also implies that less nuclear fuel is used, resulting in more compact nuclear reactors. Thus, this study aims to understand high-temperature latent heat storage systems with nanoparticles during the melting processes, in order to ensure the compactness and safety of a reactor. The study will be carried out through the use of computational tools such as computational fluid mechanics (CFD), applied to a known TES available in the open literature.*

Keywords: *Phase Change Materials, Nanofluids, Thermal Energy Storage*

1. INTRODUCTION

Although it is not the closest planet to us, Mars is considered, a compelling astrobiological target due to its similarities with earth and high life-potential. Thereby the human exploration of Mars would have the potential to bring new advances to science and prospects for future habitations for earthly life.

However, sustaining human life in a hostile environment during the transfer, stay and return to Earth-Mars is one of the most notable problems during this type of mission. Immence spacecraft would be needed to ensure safety and comfortable conditions for the crew during the travel. This results in the need for a large system and an enormous amount of uninterrupted power with a stable quality.

Solar energy is the most common and main form of energy used in space travel, however, it becomes progressively more inefficient depending on the solar flux. The alternative to solar cells is compact nuclear reactors, capable of powering the propulsion system and supply the energy demand of the other equipment, which can allow the extension of space mission, from an interplanetary exploration to spacial colonization.

Fast micro-reactors have been studied and developed as an alternative for space nuclear propulsion (Guimares *et al.*, 2011). However, considering that the reactor will provide energy for more than one purpose, variable power demand results in a significant amount of reactor stress, since these systems are generally designed to operate at a constant energy level, resulting in a robust control and safety system, and a larger reactor. The coupling of a nuclear reactor to a thermal storage system can make feasible the use of nuclear energy in power and propulsion systems. The nuclear reactor can operate at a constant power level, supplying heat to the TES (Thermal Energy Storage), which can supply the power system as required, quickly responding to demand variations without overloading the control system. The coupling suggests that less nuclear fuel is used, resulting in a smaller and lightweight reactor.

In recent years, thermal energy storage technologies have drawn attention by using phase change materials (PCMs) as an effective way of storing thermal energy with high storage density and energy (Fernandes Farias *et al.*, 2018). PCMs have been widely used in the control of heat pumps, solar engineering, and space applications. To reduce the charge/discharge time of the TES system, materials with high diffusivity can be used. However, the fluids traditionally used (water, alcohol, ethylene glycol) have low thermal diffusivity when compared to metallic solids. Therefore, to increase the thermal exchange efficiency, it is necessary to increase the available heat transfer area between the surface and the working fluid. This results in larger, heavier, and therefore more expensive systems (Wang and Mujumdar, 2007).

In order to increase the heat transfer rate without increasing equipment size, metallic solids can be dissolved in the liquids to increase the thermal conductivity of the blend. However, solutions with micro or milli solid particles have low solution stability and tend to sediment, creating a new resistance to heat transfer, which can cause erosion of the equipment. The dispersion of high conductivity nanoparticles can be a solution to improve the thermal conductivity of these PCMs. Nanoparticles, with an average size smaller than 50nm, have a contact surface larger than the micro or milli particles and greater stability of the solution. Thus the thermophysical properties can be improved (Wang and Mujumdar, 2007).

Thus, this study aims to understand the latent heat storage systems during the melting process using a high-temperature material as $NaCl$ and nanoparticles. The study will be done through the use of computational tools such as computational fluid mechanics (CFD), applied to a heat exchanger found in the open literature.

2. COMPUTATIONAL PROCEDURES

In this study, $NaCl$ will be used as a phase change material to absorb the heat supplied from the nuclear reactor. However, it has a low thermal conductivity when compared to metallic solids. In order to increase the heat transfer rate without increasing equipment size, metallic solids can be dissolved in the material (da Fonseca, 2007). Studies have been developed to predict the behavior of thermal conductivity in nanofluids, from simple correlations as described in Maxwell (1881) to complex and more detailed models. However, the model that best describes the nanofluid behavior must consider that the metallic particles not only alter the thermal conductivity but also viscosity, density, and consequently, the heat transfer capacity. In this study, the model proposed by Hamilton and Crosser (1962) is the chosen model used to compute the nanofluid thermo-physical properties as follows.

$$\frac{k_{eff}}{k_f} = \frac{k_p + (n-1)k_f \ - (n-1)\phi(k_f - k_p)}{k_p + (n-1)k_f + \phi(k_f - k_p)} \tag{1}$$

CFD is used to simulate the fluid behavior, considering the phenomena of diffusion, natural convection and phase change. Initially, a traditional workflow will be simulated in order to validate the numerical model with experimental data. To the commercial code, the physical characteristics model of nanofluids must be added, which must consider that the metallic particles not only alter the thermal conductivity, but also the viscosity, the density and, therefore, the capacity of heat transfer as described in **?**, which is used as the numerical model reference for this project.

The problems of fusion and solidification can be solved from a porosity-enthalpy formulation used to monitor the movement of the liquid-solid interface. In this technique, the fusion interface is not explicitly tracked, instead, the net fraction, which indicates the fraction of the volume of the cell that is in liquid form, is associated with each cell in the domain. The net fraction is calculated at each iteration, based on an enthalpy balance.

The mush zone is a region in which the liquid fraction is between 0 and 1 and is modeled as a porous media in which the porosity decreases from 1 to 0 as the material solidifies. When the material solidifies completely in a cell, the porosity becomes zero and therefore the velocities also fall to zero (Fluent, 2009). The enthalpy of the material is computed as the sum of the sensible enthalpy (h) and of the latent heat (ΔH), where h is defined by the eq. 2.

$$h \quad = \quad h_{ref} + \int_{Tref}^{T} c_p dT \tag{2}$$

where h_{ref} is the refence enthalpy, c_p the specific heat and T temperature.

Liquid fraction (β), can be defined by the eq. 3, if $T > T_{liquid}$, then $\beta = 1$ and if $T < T_{solid}$, then $\beta = 0$.

$$\beta \quad = \quad \frac{T - T_{solid}}{T_{liquid} - T_{solid}} \qquad if \quad T_{solid} < T < \quad T_{liquid} \tag{3}$$

This model treats density as a constant value in governing equations, except in one of the terms of the momentum equation, where the density, ρ varies with temperature and is computed taking into account a coefficient of thermal expansion, β_{exp}, according to the Boussinesq approximation as eq. 4.

$$\rho \quad = \quad \rho_i \left(1 - \beta_{exp} \cdot \Delta T\right) \tag{4}$$

The latent heat content can now be written in terms of the latent heat of the material, according to eq. 5, where the latent heat can vary from 0 when solid and L when liquid.

$$\Delta H = \beta L \tag{5}$$

For the melting and solidification process, the energy equation reduces to eq. 6, where $\vec{v}$ is the velocity of the fluid, S is the source term and ρ density. Thus, the solution for temperature is essentially an interaction between the energy equation and the liquid fraction equation.

$$\frac{\partial}{\partial t}\left(\rho H\right) + \nabla \cdot \left(\rho \vec{v} H\right) = \nabla \cdot \left(k \nabla T\right) + S \tag{6}$$

For solidification and melting of a pure substance, the phase change occurs at a different melting temperature T_{melt}. For a multicomponent mixture, however, there is a pasty solidification/melting zone between low solid temperature and high liquid temperature. When a multicomponent liquid solidifies, the solutes diffuse from the solid phase to the liquid phase.This effect is quantified by the partition coefficient of the solute, denoted by K_i, which is the ratio of the mass fraction in the solid to the liquid in the interface (Maliska, 2001). The temperature of the liquid and the solid in a mixture can be calculated as:

$$T_{solid} = T_{melt} + \sum m_i Y_i / K_i \tag{7}$$

$$T_{liquid} = T_{melt} + \sum m_i Y_i \tag{8}$$

where, Y_i is the mass fraction of the solute, and m_i is the inclination of the liquid surface in relation to Y_i.

Considering a given volume V of the fluid mixture, and letting M_i be the mass of the component *i* present in this volume, then $\rho_i = M_i/V$. The partial volume of the component *i* is defined as the volume, V_i, which would be occupied by the given mass of the component at the same localized temperature and pressure of the mixture. The thermodynamic density of the component, which results from the evaluation of its state equation in the temperature and pressure of the mixture, can be expressed as $\langle \rho_i \rangle = M_i/V_i$.

The partial volumes of all the components must add up to the volume, V. The multi-fluid equation is given by the following equation.

$$\frac{1}{\rho} = \sum Y_i / \langle \rho_i \rangle . \tag{9}$$

Thus, the density of the blend can be calculated by the mass fraction and the thermodynamic density of the component. The density component ρ_i, is related to the composition of the blend while $\langle \rho_i \rangle$, is the properties of the material. The enthalpy-porosity model treats the soft region (partially solidified region) as a porous medium. The porosity in each cell is equal to the net fraction in that cell. In fully solidified regions, the porosity is equal to zero, extinguishing the velocity profile in this region. Thus, the equation of the moment is reduced by the following form:

$$S = \frac{(1-\beta)^2}{(\beta^3+\varepsilon)} A_{mush} \left(\overrightarrow{v} - \overrightarrow{v}_p \right) \tag{10}$$

where ε is a negligible number used to avoid division by zero, A_{mush} is the constant of the soft zone, $\overrightarrow{v}_p$ is the velocity of the solid due to the inertia of the solidified material out of the domain (also known as the traction velocity). The mush zone constant measures the damping amplitude, the higher this value, the steeper the material velocity transition to zero as it solidifies, too large values can cause the solution to oscillate. Numerical analysis is performed using the Finite Volume Method for volume control, treating the fluid as incompressible, as described in Maliska (2001).

The SIMPLE method was used to solve the governing equations. The time interval for integrating the time derivatives was set to 1 s. The differentiation scheme *Second Order Upwind* was used to evaluate the convective flow on the faces of the control volumes, while the SIMPLE scheme was adopted for the pressure correction equation. Where the governing equations are described as follows, in Equation (11) mass conservation, the momentum conservation Equations (12, 13 and 14) and the energy Equation 15. Where, u, v and w refer to the velocities in the directions x, y and z and **u** is the vector of microscopic velocity, S is the source term, as described in malalasekera1995introduction.

$$\nabla \cdot (\mathbf{u}) = 0 \tag{11}$$

$$\frac{\partial(\rho u)}{\partial t} + \nabla \cdot (\rho u \mathbf{u}) = -\frac{\partial p}{\partial x} + \nabla \cdot (\mu \nabla u) + S_{Mx} \tag{12}$$

$$\frac{\partial(\rho v)}{\partial t} + \nabla \cdot (\rho v \mathbf{u}) = -\frac{\partial p}{\partial y} + \nabla \cdot (\mu \nabla v) + S_{My} \tag{13}$$

$$\frac{\partial(\rho w)}{\partial t} + \nabla \cdot (\rho w \mathbf{u}) = -\frac{\partial p}{\partial z} + \nabla \cdot (\mu \nabla w) + S_{Mz} \tag{14}$$

$$\frac{\rho c_p T}{\partial t} + \nabla \cdot (\rho c_p T \mathbf{u}) = -p \nabla \cdot (u) + \nabla \cdot (k \nabla T) + \Phi + S_i \tag{15}$$

3. RESULTS

In reason to evaluate the $NaCl$ discharge cycles of a latent heat storage unit (LHS), as described in Farias and Ribeiro (2019), through computational models. The LHS unit includes a Shell-and-tube and $NaCl$ heat exchanger as thermal energy storage material, which can be enhanced with the use of different nano-additives.

In this study, the heat exchanger is made of copper. The outer diameter, the length and the thickness of the shell are 450 mm, 385 mm and 1 mm, respectively. Likewise, the outside diameter and the thickness of the tubes are 22 mm and 1 mm. The longitudinal fins are connected to tubes of length, width and thickness of 230 mm, 40 mm and 1.5 mm, respectively. The 50 mm thick chlorofluorocarbon-free wire insulation is cushioned around the outer surface of the enclosure to minimize thermal losses as shown in Figure 1.

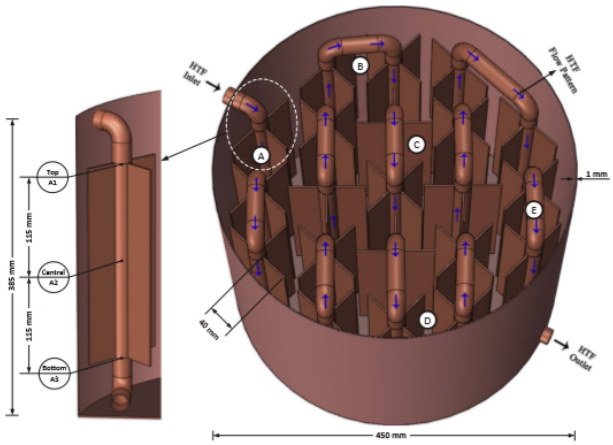

Figure 1. Benchmark shell-and-tube heat exchanger.

During the loading phase, the $NaCl$ is initially in a solid state, so its initial temperature must be smaller than the melting point, which is 1072K. During this phase, the pipe wall is maintained at a fixed temperature of $1090K$, transferring heat to the solid that will change phase until its complete fusion when it reaches thermal balance.

In the same line, we will evaluate the effect of the change of the properties of $NaCl$ by adding different concentrations of nanofluids to the material of phase change. For the given analysis, we will use the following properties of nanofluids.

Table 1. Properties of nanoparticles.

Material	ρ **(kg/**m^3**)**	C_p **(kJ/kg.K)**	k_{eff} **(W/mK)**
CuO	6500	536	20
Al_2O_3	3900	880	42

As can be seen in Figs. 2 and 4, Alumina presents a better performance reducing loading time in relation to copper oxide, due to the increase in thermal diffusivity, which showed an increase of up to 6.77 % for 5 % of alumina when compared to copper oxide. The thermal diffusivity increases the thermal dissipation in the material, thus the PCM $NaCl-Al_2O_3$ reaches higher temperatures in a shorter period of time, for materials with 5 % volume addition.

To reach 90 % of the volume of the PCM in liquid state, with pure base it takes 145 seconds, a time that can be reduced by 3, 8 and 12% by adding Al_2O_3 in volumetric fractions of 1, 3 and 5 %. For the same volumetric fraction, adding CuO time reduces by 2, 6 and 10%.

Figure 4 presents the temperature lines at point B-top displayed in Fig. 1, where initially the effect of nanofluids, up to the phase change temperature, is less relevant, since the addition of 5% de Al_2O_3 reduces in only 3% the time it takes the PCM to reach a temperature of 1072 K. However, after reaching the melting temperature, a greater dissociation of the curves up to the equilibrium temperature of 1090 K can be seen in the results, due to the dependence of thermal properties with temperature leads to an increase in thermal diffusion. In the lower right corner of the Fig. 4 there is an enlargement of the graph for the time quadrant between 200 and 250 seconds, where the detachment of the lines is more representative.

By the same token, Fig.5 shows the temperature lines at the point B-top, where initially the addition of 5% CuO reduces by only 2 % the time that the PCM takes to reach the temperature of 1072 K.

Another point worth mentioning is the mass and time product of the nanofluids. As can be seen in Fig. 6, the behavior of the product average mass and melting time of CuO is different from that of alumina. While copper oxide has an increasing function, indicating that the increase in mass has a greater influence on the PCM than the reduction in melting time. For alumina the situation is opposite, presenting a decreasing function where the influence of mass reduction is

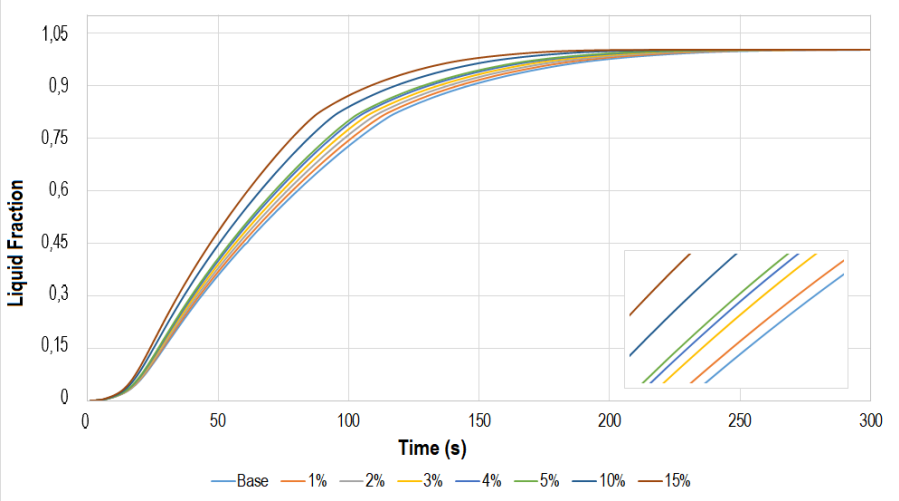

Figure 2. Liquid Fraction change over time for the nanofluid $NaCl$-Al_2O_3.

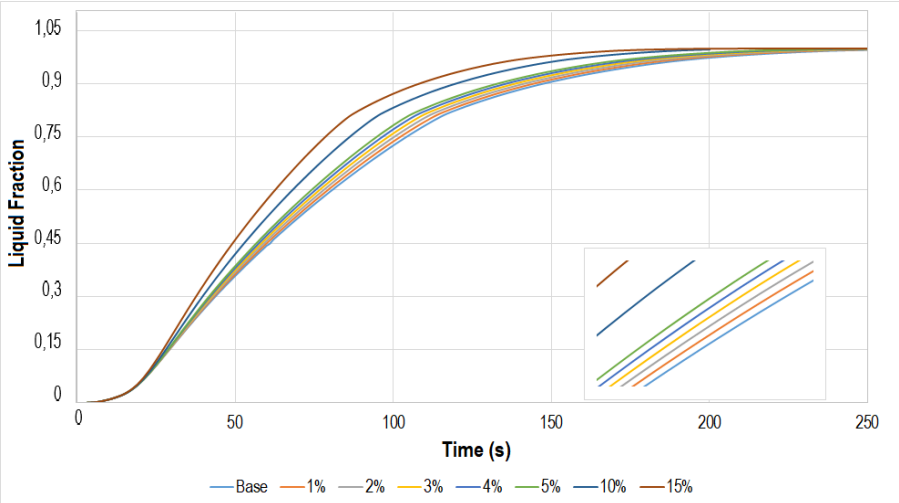

Figure 3. Liquid Fraction change over time for the nanofluid $NaCl$-CuO.

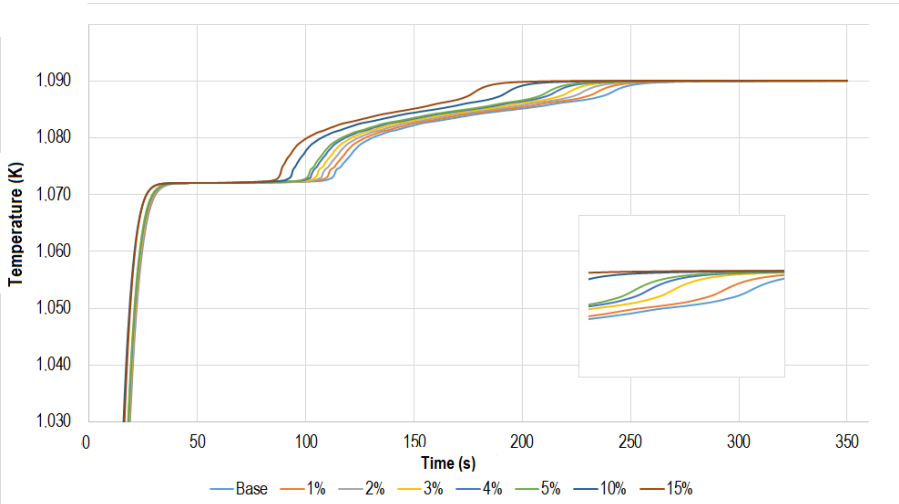

Figure 4. Temperature change (K) of the PCM with the addition of Al_2O_3.

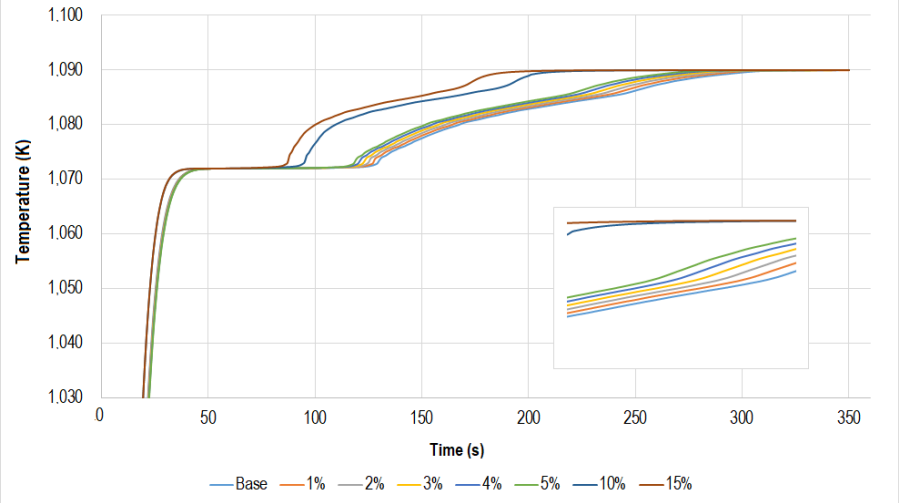

Figure 5. Temperature change (K) of the PCM with the addition of CuO.

stronger.

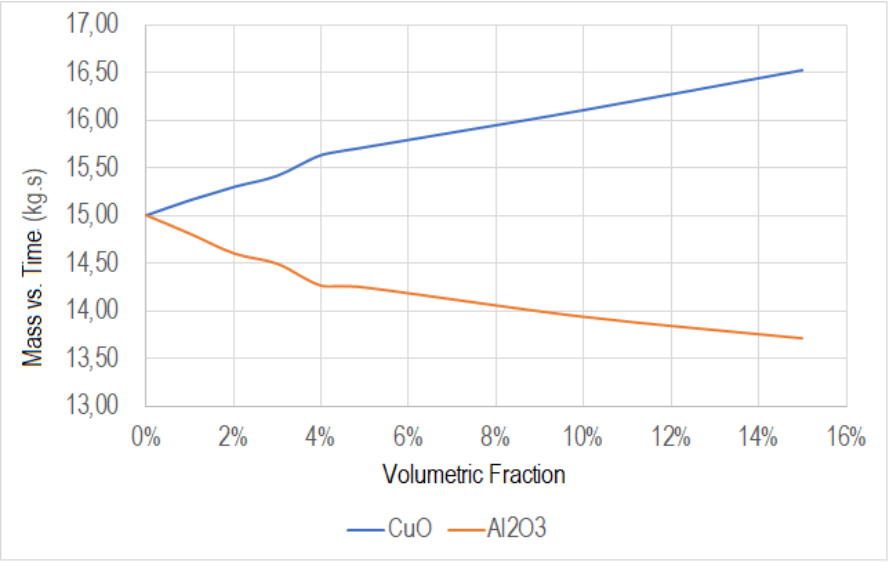

Figure 6. Variation of product mass *vs.*. time reduction.

For the $NaCl - CuO$ nanofluid, it is observed that the increase in concentration from 3 to 4% results in a smaller percentage reduction (1.5%) in the melting time compared to the results of 2-3% and 4-5%. When looking at Fig. 6, for CuO the variation of the product $m.t$ rises 1.4% in the volume fraction of 3-4%, presenting the highest increase in the interval. The point of least growth of the product is for the concentration of 5 % that presents 0.5% of growth. Therefore, the use of $NaCl - CuO$ nanofluid is not justified in the application of compact and lightweight TES, where mass reduction is relevant.

This same lag can be seen for the alumina nanofluid, because when adding the concentration from 4 to 5%, the time reduction drops from 3% to 1.5%. For alumina, the ideal concentration is 4%, as it presents the greatest percentage reduction in melting time and the greatest reduction in the product $m.t$, indicating that alumina is indicated in the application of compact TES.

4. Conclusions

This work was developed with the main objective of contributing to the development of nuclear reactors, by introducing thermal storage technology in the energy conversion system, aiming to reduce the stress applied in the reactor control system, which can operate at a lower power. and more constant, increasing the safety of the project and reducing the final

mass of nuclear fuel.

The study is developed from the simulation of a heat exchanger with a high temperature phase change material, suitable for the operating temperature of a nuclear reactor.

When using a high temperature material, such as $NaCl$, the performance of alumina proved to be much superior to the performance presented by copper oxide. The increase in specific mass in the $NaCl - CuO$ nanofluid becomes very relevant for the definition of thermal properties, which directly affects the performance of the heat exchanger.

For the $NaCl - CuO$ nanofluid, it is observed that again the increase in the mass of the nanofluid is less than the reduction in the melting time. Therefore, the use of $NaCl - CuO$ nanofluid is not justified in the application of compact TES. However, for alumina, when the concentration of nanoparticles rises from 4-5%, the time reduction drops from 3 % to 1.5 %, indicating that for alumina, the ideal concentration is 4 %, since it presents the greatest percentage reduction in melting time and the greatest reduction in the product mt. Thus, the use of alumina in $NaCl$ is indicated in the application of compact TES in high temperature space applications.

In general, the results obtained in this work are encouraging for the continuity of the study of the application of nanofluids in thermal storage with spatial systems.

5. REFERENCES

da Fonseca, H.M., 2007. *Caracterização termofísica de nanofluidos*. Ph.D. thesis, UNIVERSIDADE FEDERAL DO RIO DE JANEIRO.

Farias, C.F. and Ribeiro, G.B., 2019. "Cfd analysis of a compact thermal energy storage system with a phase change material". *XXI ENFIR - Meeting on Nuclear Reactor Physics and Thermal Hydraulics*.

Fernandes Farias, C., Ribeiro, G. and José dos Santos de Lemos, M., 2018. "Heat transfer in channels using nanofluids, porous media and the two energy equation model".

Fluent, A., 2009. "12.0 theory guide". *Ansys Inc*, Vol. 5, No. 5.

Guimares, L., Camillo, G., Placco, G., Barrios, G., Do Nascimento, J., Borges, E., De Castro Lobo, P. *et al.*, 2011. "Basic research and development effort to design a micro nuclear power plant for brazilian space applications". *Journal of the British Interplanetary Society*, Vol. 64, pp. 194–199.

Hamilton, R. and Crosser, O., 1962. "Thermal conductivity of heterogeneous two-component systems". *Industrial & Engineering chemistry fundamentals*, Vol. 1, No. 3, pp. 187–191.

Maliska, C.R., 2001. "Issues on the integration of cfd to building simulation tools". *ISSUES*.

Maxwell, J.C., 1881. *A treatise on electricity and magnetism*, Vol. 1. Clarendon press.

Wang, X.Q. and Mujumdar, A.S., 2007. "Heat transfer characteristics of nanofluids: a review". *International journal of thermal sciences*, Vol. 46, No. 1, pp. 1–19.

6. RESPONSIBILITY NOTICE

The authors are solely responsible for the printed material included in this paper.